

Mollified Hyperbolic Method for Coefficient Identification Problems

C. E. MEJÍA AND D. A. MURIO

University of Cincinnati, Department of Mathematical Sciences
Cincinnati, OH 45221-0025, U.S.A.

(Received March 1999; accepted April 1999)

Abstract—We introduce a stable numerical method for the identification of a transmissivity coefficient in a one-dimensional parabolic equation. It is a combination of the Mollification Method and a well-known space marching implementation of the Hyperbolic Regularization procedure. The new method successfully restores a certain type of continuity with respect to the initial condition and the boundary data. The accuracy of the algorithm is demonstrated by means of several examples where exact and perturbed data are considered.

1. INTRODUCTION

Many physical models include undetermined coefficients in the equations and the solution of the inverse problems consisting of the identification of these coefficients has become a very active area of research in recent years. In particular, a variety of problems in reservoir simulation, flow in porous media, heat conduction, chemical kinetics, population dynamics, and other areas, propose the identification of coefficients in parabolic equations. For a detailed treatment of some of these problems, consult [1,2], and the references therein.

In [3,4], Ewing and Lin consider a simplified model of single-phase flow and instead of following the commonly used least squares methods of “History Matching,” they developed an easy to implement algorithm based on a space marching scheme of finite difference equations. They proved a general error estimate that allows for perturbations in the boundary data, but clearly stated that the numerical method relies on exact initial data in order to be successful.

In this paper, we enhance the method of Ewing and Lin with the desirable feature of allowing perturbations in the boundary data as well as in the initial conditions. Our approach is the use of a filtering procedure known as the Mollification Method. Roughly speaking, the mollification of a perturbed function restores stability by damping the high frequency Fourier components of the perturbation. A complete description of this method and several of its applications can be found in [5].

Section 2 introduces the regularization procedure used by Ewing and Lin to stabilize the identification problem.

Section 3 presents the Mollification Method and explains the combination of the two regularization procedures. The main feature of this section is Proposition 3, which explains the automatic extension procedure that we developed in order to compute the convolution that defines the mollification throughout the entire domain of definition of the partial differential equation and not only on a compact subset, as is usually the case.

Both authors were partially supported by a C. Taft Fellowship and a University Research Council Summer Fellowship.

Typeset by *AMS-T_EX*

In Section 4, we describe the numerical scheme and present two stability estimates. The first one takes into account the presence of the two regularization procedures. The second one, developed by Ewing and Lin in [3], is included for completeness and to show the way the mollification reveals itself in its error bound.

Several examples are presented in detail in Section 5, as well as a few considerations of practical importance.

2. HYPERBOLIC REGULARIZATION

Ewing and Lin [3] consider a single-phase flow in a radially homogeneous medium. The parameter identification problem is the following:

Identify the coefficient $a(x)$, $0 \leq x \leq 1$, in

$$\begin{aligned} u_t &= (au_x)_x + f(x, t), & 0 < x < 1, 0 < t, \\ u(x, 0) &= g(x), & 0 < x < 1, \\ u(0, t) &= \psi(t), & 0 < t, \\ u_x(0, t) &= \phi(t), & 0 < t. \end{aligned} \tag{1}$$

Because of the ill-posedness of inverse problems in general and of parameter estimation problems in particular, a regularization is necessary. Ewing and Lin modify system (1) as follows:

$$\begin{aligned} \gamma^2 u_{tt} + u_t &= (au_x)_x + f(x, t), & 0 < x < 1, 0 < t, \\ u(x, 0) &= g(x), & 0 < x < 1, \\ u(0, t) &= \psi(t), & 0 < t, \\ u_x(0, t) &= \phi(t), & 0 < t, \\ u_t(x, 0) &= (a(x)u_x(x, 0))_x + f(x, 0), & 0 < x < 1, \end{aligned} \tag{2}$$

where γ , the parameter of regularization, is a positive constant.

This stabilization is called Hyperbolic Regularization; it has been used for the solution of a variety of inverse problems. (See [4,6,7]). For the numerical solution of the new problem, Ewing and Lin developed an explicit finite difference space marching numerical scheme, and proved its stability with respect to the data on the boundary $x = 0$, assuming g is known exactly.

We think that to restore stability with respect to the data for $t = 0$ would be a desirable feature for this method. The main difficulty is the division by an approximation of the derivative of the initial data. In order to address this difficulty, we modify problem (2) a little further by introducing the Mollification Method.

3. MOLLIFICATION

The Mollification Method is a regularization procedure for Ill-Posed problems; its description and several of its applications can be found in [5]. Reference [8] is a complete description of the use of the Mollification Method for the regularization of numerical differentiation.

We use the Gaussian Kernel

$$\rho_\delta(t) = \frac{1}{\delta\pi^{1/2}} \exp\left(\frac{-t^2}{\delta^2}\right)$$

as mollifier and define the δ -mollification of a function $f(t)$ by

$$J_\delta f(t) = (\rho_\delta \star f)(t) = \int_{-\infty}^{\infty} \rho_\delta(t-s)f(s) ds.$$

$J_\delta f(t)$, the one-dimensional convolution of ρ_δ and f , is a C^∞ function. The mollifier $\rho_\delta(t)$ is positive, falls to nearly zero outside $[-3\delta, 3\delta]$ and its total integral is 1. If $f(t)$ is sufficiently smooth, $|J_\delta f(t) - f(t)| \rightarrow 0$ and $|J_\delta f'(t) - f'(t)| \rightarrow 0$ as $\delta \rightarrow 0$. More precisely:

PROPOSITION 1. (*Consistency*). If $f(t) \in C^2(D)$, $D \subset R$, then there exists a constant C independent of δ such that

$$\|J_\delta f - f\|_{\infty, D} \leq C\delta \quad \text{and} \quad \|J_\delta f' - f'\|_{\infty, D} \leq C\delta. \quad (3)$$

PROOF. See [5]. ■

If we only know a measured approximation $f_m(t)$ of $f(t)$ and a tolerance $\epsilon > 0$ such that $\|f - f_m\|_{\infty, D} \leq \epsilon$, then we have the following stability estimates.

PROPOSITION 2. (*Stability*). If $f_m(t) \in C^0(D)$ and $\|f - f_m\|_{\infty, D} \leq \epsilon$, then

$$\|J_\delta f - J_\delta f_m\|_{\infty, D} \leq \epsilon \quad \text{and} \quad \|(J_\delta f)' - (J_\delta f_m)'\|_{\infty, D} \leq \left(\frac{2}{\sqrt{\pi}}\right) \frac{\epsilon}{\delta}. \quad (4)$$

PROOF. See [5]. ■

If D is a bounded interval with end points a and b , the convolution $\rho_\delta \star f$ requires either the extension of f to a slightly bigger set $D' \supset D$ or the consideration of f restricted to a suitable compact set $K \subset D$. Both sets, D' and K , depend on δ . Our approach is the first one, and we restrict our attention to the end point b to present the details.

Assume $\rho_\delta(t) = 0$ if $|t| > 3\delta$. We seek extensions \tilde{f} of f to the domain $[a, b + 3\delta]$, satisfying the condition

$$\|J_\delta(\tilde{f}) - f\|_{L^2[b-3\delta, b]} \text{ is minimum.}$$

If we require \tilde{f} to be a constant on $(b, b + 3\delta]$, we obtain a unique solution to this problem by the following optimization procedure.

PROPOSITION 3. Suppose $f(t) \in L^2([a, b])$. There exists a constant c such that if $f(t)$ is extended by letting $f(t) = c$ for all $t \in [b, b + 3\delta]$, then $\|J_\delta(f) - f\|_{L^2[b-3\delta, b]}$ is minimum.

PROOF. The real function

$$\begin{aligned} \mathcal{F}(c) &= \|J_\delta(f) - f\|_{L^2[b-3\delta, b]}^2 \\ &= \int_{b-3\delta}^b \left[\left(\int_{-\infty}^{\infty} \rho_\delta(s) f(t-s) ds \right) - f(t) \right]^2 dt \\ &= \int_{b-3\delta}^b \left[\int_a^b \rho_\delta(t-s) f(s) ds + \int_b^{b+3\delta} c \rho_\delta(t-s) ds - f(t) \right]^2 dt, \end{aligned}$$

achieves its minimum value at

$$c = \frac{\int_{b-3\delta}^b \left[f(t) - \int_a^b \rho_\delta(t-s) f(s) ds \right] \left[\int_b^{b+3\delta} \rho_\delta(t-s) ds \right] dt}{\int_{b-3\delta}^b \left[\int_b^{b+3\delta} \rho_\delta(t-s) ds \right]^2 dt}. \quad (5) \quad \blacksquare$$

REMARKS.

- We omit the similar results for the other end of the interval.
- Other extensions of the function f , for instance, polynomial extensions of higher degree, are also possible, but we do not consider them here.
- In computations, we have only discrete functions. The actual value of the constant c is obtained from (5) by a Rectangle Rule or other simple Quadrature Formula.

We assume that the boundary and the initial data for Problem (1) are obtained from measurements. That is, there are C^0 functions $g_m(x)$, $\psi_m(t)$ and $\phi_m(t)$ and a positive tolerance ϵ satisfying

$$\|g - g_m\|_\infty \leq \epsilon, \quad \|\psi - \psi_m\|_\infty \leq \epsilon \quad \text{and} \quad \|\phi - \phi_m\|_\infty \leq \epsilon. \quad (6)$$

The combination of the Hyperbolic Regularization and the Mollification Method for Problem (1) with measured data, leads us to the consideration of the following problem.

Identify $a(x)$, $0 < x < 1$, in

$$\begin{aligned} \gamma^2 u_{tt} + u_t &= (au_x)_x + f(x, t), & 0 < x < 1, 0 < t, \\ u(x, 0) &= J_\delta g_m(x), & 0 < x < 1, \\ u(0, t) &= J_\delta \psi_m(t), & 0 < t, \\ u_x(0, t) &= J_\delta \phi_m(t), & 0 < t, \\ u_t(x, 0) &= (a(x)u_x(x, 0))_x + f(x, 0), & 0 < x < 1, \end{aligned} \quad (7)$$

where δ is the radius of mollification, $J_\delta g_m(x)$ is the mollification in x of $g_m(x)$, and $J_\delta \psi_m(t)$ and $J_\delta \phi_m(t)$ are the mollifications in t of $\psi_m(t)$ and $\phi_m(t)$, respectively.

4. NUMERICAL SCHEME

We apply the numerical scheme of Ewing and Lin to Problem (7). Here we restrict ourselves to present only a brief sketch of the marching scheme. For a detailed discussion, see [3].

4.1. Discretization

Let M and N be positive integers, $h = \frac{1}{M}$, $k = \frac{1}{N}$, $x_j = jh$, $j = 0, 1, \dots, M$, $t_n = nk$, $n = 0, 1, \dots$. We denote $v(x, t) = u_x(x, t)$ and $w(x, t) = \gamma u_t(x, t)$. For $n \geq 0$, let

$$\begin{aligned} f_j^n &= f(jh, nk), & j \geq 0 \\ G_j &= J_\delta g_m(jh), & j \geq 0 \\ g_j &= g(jh), & j \geq 0 \\ u_0^n &= \psi(nk) \\ v_{1/2}^n &= \phi(nk) \\ w_0^n &= \gamma \psi'(nk) \\ v_{j+1/2}^n &= v\left(\left(j + \frac{1}{2}\right)h, nk\right), & j \geq 1 \\ w_j^n &= w(jh, nk), & j \geq 1 \\ a_{j+1/2} &= a\left(\left(j + \frac{1}{2}\right)h\right), & j \geq 0. \end{aligned}$$

Let the variables of the numerical method be U_j^n , V_j^n , W_j^n and A_j . They are discrete functions defined on the grid with discretization steps h and k . Their starting values are given for all n in order to proceed with a space marching scheme. They are:

$$\begin{aligned} U_0^n &= J_\delta \psi_m(nk) \\ V_{1/2}^n &= J_\delta \phi_m(nk) \\ W_0^n &= \gamma (J_\delta \psi_m)'(nk) \\ A_{1/2} &= a\left(\frac{1}{2}h\right) \\ U_1^n &= U_0^n + hV_{1/2}^n. \end{aligned}$$

We point out that, with the exception of the starting value $A_{1/2}$ which is exact, we use only measured data conveniently filtered by the Mollification procedure. However, stability estimates do not require $A_{1/2}$ to be exact and calculations reveal that an educated guess for $A_{1/2}$ is also a feasible alternative.

The space marching scheme of Ewing and Lin for the solution of Problem (1) is defined by the equations

$$A_{j+1+1/2} = \frac{1}{G_{j+2} - G_{j+1}} \left\{ A_{j+1/2} (G_{j+1} - G_j) + h^2 \left(\frac{U_{j+1}^1 - G_{j+1}}{k} - f_{j+1}^0 \right) \right\}, \quad (8)$$

$$U_{j+1}^n = U_j^n + \frac{1}{A_{j+1/2}} \left\{ A_{j-1/2} (U_j^n - U_{j-1}^n) + h^2 \left(\gamma^2 \frac{U_j^{n+1} - 2U_j^n + U_j^{n-1}}{k^2} + \frac{U_j^{n+1} - U_j^{n-1}}{2k} - f_j^n \right) \right\}, \quad (9)$$

which in terms of the other variables are

$$\frac{A_{j+1+1/2}(G_{j+2} - G_{j+1}) - A_{j+1/2}(G_{j+1} - G_j)}{h^2} = \frac{1}{\gamma} W_{j+1}^0 - f_{j+1}^0, \quad (10)$$

$$\frac{A_{j+1+1/2} V_{j+1+1/2}^n - A_{j+1/2} V_{j+1/2}^n}{h} = \frac{\gamma}{k} (W_{j+1}^n - W_j^n) + \frac{1}{\gamma} W_{j+1}^n - f_{j+1}^n. \quad (11)$$

The calculations are performed in a triangular region in the (x, t) -plane. A sufficient amount $L + 1$ of point values of the boundary data at $x = 0$ should be read in order to be able to recover not only the values of the coefficient a , but also the solution u and its first derivatives u_t and u_x for $0 < x < 1$ and $0 < t < T$. We assume $(L + 1)k = \eta T$, where η is a constant.

4.2. Analysis

In this section, we prove a stability estimate for the recovery of the diffusivity coefficient that takes into consideration the presence of noise in the initial data. We base our proof on virtually the same assumptions Ewing and Lin require for their analysis. A summary of this analysis and their main result are also presented.

We start with the definition of the error functions:

$$\begin{aligned} \Delta V_{j+1/2}^n &= v_{j+1/2}^n - V_{j+1/2}^n, \\ \Delta W_j^n &= w_j^n - W_j^n, \\ \Delta A_{j+1/2} &= a_{j+1/2} - A_{j+1/2}, \end{aligned}$$

and with the assumptions that are necessary in order to carry out the error analysis.

ASSUMPTION 1. $g(x) \in C^2([0, 1])$ and there exist positive constants M_0 and M_1 such that

$$\begin{aligned} M_0 &\leq \inf_{x \in [0, 1]} |g'(x)| \leq \sup_{x \in [0, 1]} |g'(x)| \leq M_1, \\ M_0 &\leq \inf_{x \in [0, 1]} |J_\delta g'(x)| \leq \sup_{x \in [0, 1]} |J_\delta g'(x)| \leq M_1, \\ M_0 &\leq \inf_{x \in [0, 1]} |(J_\delta g_m)'(x)| \leq \sup_{x \in [0, 1]} |(J_\delta g_m)'(x)| \leq M_1. \end{aligned}$$

ASSUMPTION 2. There are positive constants M_2 and M_3 such that

$$\begin{aligned} M_2 &\leq \inf_{x \in [0, 1]} a(x) \leq \sup_{x \in [0, 1]} a(x) \leq M_3, \\ M_2 &\leq \min_j A_{j+1/2} \leq \max_j A_{j+1/2} \leq M_3, \quad \max_j |W_j^0| \leq M_3. \end{aligned}$$

ASSUMPTION 3. $u(x, t) \in C^2([0, 1] \times [0, T])$. In particular, there exists a positive constant M_4 such that

$$|u_t(x, t)| \leq M_4.$$

Now we present the error estimate for the diffusivity coefficient that uses equation (10) as the starting point, and therefore, depends heavily on the presence of noise in the initial data $g(x)$.

THEOREM 4. If Assumptions 1–3 are satisfied, then there exists a constant M_5 such that

$$|\Delta A_{j+1/2}| \leq \left(\frac{M_1}{M_0}\right)^M |\Delta A_{1/2}| + M_5 \left(\delta + \frac{\epsilon}{\delta} + h + \frac{h}{\gamma}\right) \left(\sum_{i=0}^M \left(\frac{M_1}{M_0}\right)^i\right). \quad (12)$$

PROOF. By expanding v, w and a at the grid points, we have

$$\frac{a_{j+1+1/2}(g_{j+2} - g_{j+1}) - a_{j+1/2}(g_{j+1} - g_j)}{h^2} = \frac{1}{\gamma} w_{j+1}^0 - f_{j+1}^0 + O(h^2),$$

and (10) says

$$\frac{A_{j+1+1/2}(G_{j+2} - G_{j+1}) - A_{j+1/2}(G_{j+1} - G_j)}{h^2} = \frac{1}{\gamma} W_{j+1}^0 - f_{j+1}^0.$$

We subtract and obtain

$$\begin{aligned} \frac{1}{h} \left\{ a_{j+1+1/2} \left(\frac{g_{j+2} - g_{j+1}}{h} \right) - A_{j+1+1/2} \left(\frac{G_{j+2} - G_{j+1}}{h} \right) - a_{j+1/2} \left(\frac{g_{j+1} - g_j}{h} \right) \right. \\ \left. + A_{j+1/2} \left(\frac{G_{j+1} - G_j}{h} \right) \right\} = \frac{1}{\gamma} (w_{j+1}^0 - W_{j+1}^0) + O(h^2). \end{aligned}$$

This implies

$$\begin{aligned} \Delta A_{j+1+1/2} \left(\frac{G_{j+2} - G_{j+1}}{h} \right) &= \Delta A_{j+1/2} \left(\frac{G_{j+1} - G_j}{h} \right) \\ &+ a_{j+1+1/2} \left(\frac{G_{j+2} - G_{j+1}}{h} - \frac{g_{j+2} - g_{j+1}}{h} \right) \\ &+ a_{j+1/2} \left(\frac{g_{j+1} - g_j}{h} - \frac{G_{j+1} - G_j}{h} \right) + \frac{h}{\gamma} (w_{j+1}^0 - W_{j+1}^0) \\ &+ O(h^2). \end{aligned}$$

Now we use the Mean Value Theorem and Assumptions 1 and 2 to get

$$\begin{aligned} |\Delta A_{j+1+1/2}| M_0 &\leq |\Delta A_{j+1/2}| M_1 + M_3 |(J_\delta g_m)'((j+1)h) - g'((j+1)h)| \\ &+ M_3 |g'(jh) - (J_\delta g_m)'(jh)| + \frac{h}{\gamma} |w_{j+1}^0 - W_{j+1}^0| + O(h), \end{aligned}$$

which, by application of Propositions 1 and 2, and Assumptions 2 and 3, yields

$$|\Delta A_{j+1+1/2}| M_0 \leq |\Delta A_{j+1/2}| M_1 + 2M_3 \left(C\delta + \frac{2}{\sqrt{\pi}} \frac{\epsilon}{\delta} \right) + \frac{h}{\gamma} (M_3 + M_4) + O(h).$$

This expression clearly indicates the existence of a constant M_5 such that

$$|\Delta A_{j+1+1/2}| \leq \frac{M_1}{M_0} |\Delta A_{j+1/2}| + M_5 \left(\delta + \frac{\epsilon}{\delta} + h + \frac{h}{\gamma} \right),$$

and by iteration of this inequality we obtain the desired result. ■

The second error estimate, developed by Ewing and Lin in [3], uses the following norms:

$$\begin{aligned}\|\Delta V_{j+1/2}\|^2 &= \sum_{n=1}^{L-j} |\Delta V_{j+1/2}^n|^2, \\ \|\Delta W_j\|^2 &= \sum_{n=0}^{L-j} |\Delta W_j^n|^2,\end{aligned}$$

and

$$\|\Delta_j^\delta\|_k^2 = \|\Delta V_{j+1/2}\|^2 k + \|\Delta W_j\|^2 k + |\Delta A_{j+1/2}|^2. \quad (13)$$

The error bound in the next theorem, depends on h, k, γ and $\|\Delta_0^\delta\|_k$, which is the error at $x = 0$. Since $\|\Delta_0^\delta\|_k$ reflects the modifications introduced in this work, we consider it in detail.

PROPOSITION 5.

$$\|\Delta_0^\delta\|_k^2 \leq |\Delta A_{1/2}|^2 + M_6 T \left((\delta + \epsilon)^2 + \gamma \left(\delta + \frac{\epsilon}{\delta} \right)^2 \right), \quad (14)$$

where M_6 is a constant independent of δ, ϵ , and γ .

PROOF. The proof is an estimate of the first two terms of the error and is based on the consistency and stability of the mollification of the boundary data.

$$\begin{aligned}\|\Delta V_{1/2}\|^2 k + \|\Delta W_0\|^2 k &= \sum_{n=1}^L |\Delta V_{1/2}^n|^2 k + \sum_{n=0}^L |\Delta W_0^n|^2 k \\ &= \sum_{n=1}^L |v_{1/2}^n - V_{1/2}^n|^2 k + \sum_{n=0}^L |w_0^n - W_0^n|^2 k \\ &= \sum_{n=1}^L |\phi(nk) - J_\delta \phi_m(nk)|^2 k \\ &\quad + \sum_{n=0}^L |\psi'(nk) - (J_\delta \psi_m)'(nk)|^2 \gamma k.\end{aligned}$$

Propositions 1 and 2 provide the following estimation for this sum:

$$\begin{aligned}\|\Delta V_{1/2}\|^2 k + \|\Delta W_0\|^2 k &\leq k \sum_{n=1}^L (C\delta + \epsilon)^2 + \gamma k \sum_{n=0}^L \left(C\delta + \frac{2}{\sqrt{\pi}} \frac{\epsilon}{\delta} \right)^2 \\ &\leq kL(C\delta + \epsilon)^2 + \gamma k(L+1) \left(C\delta + \frac{2}{\sqrt{\pi}} \frac{\epsilon}{\delta} \right)^2 \\ &\leq M_6 T \left((\delta + \epsilon)^2 + \gamma \left(\delta + \frac{\epsilon}{\delta} \right)^2 \right),\end{aligned}$$

and from here, estimate (14) follows. ■

THEOREM 6. *If Assumptions 1–3 hold, and h and k satisfy*

$$\frac{\gamma h}{k} < \min \{M_2, M_7, 1\} \text{ and } \frac{k}{h} \leq M_6$$

for some nonzero M_6 and M_7 , then there exist nonzero constants M_8 and M_9 such that

$$\|\Delta_{j+1}^\delta\|_k^2 \leq \left(\|\Delta_0^\delta\|_k^2 + O(k) + O(h) + \gamma^2 \right) (M_8 + hC(h, k, \gamma) \exp(C(h, k, \gamma))),$$

where $C(h, k, \gamma) = M_9(1/\gamma + 1 + O(h) + O(k))$.

PROOF. See [3]. ■

REMARK. Our error estimate, Theorem 4, depends on the newly implemented feature, i.e., a noisy initial data at $t = 0$. Ewing and Lin use a well-crafted application of the Energy Method to prove their general estimate, Theorem 6, that reports errors in u_t, u_x and a simultaneously. The error bound depends primarily on h, k, γ and $\|\Delta_0^\delta\|_k$, and through $\|\Delta_0^\delta\|_k$, on δ, γ , and ϵ in the way Proposition 5 indicates.

5. NUMERICAL RESULTS

In this section, we discuss the implementation of the numerical scheme developed in the last section and present the numerical results obtained from three examples. In all the examples, the discretization parameters are the following: $M = N = 200$, $h = k = \frac{1}{M}$, $x_j = jh$, $j = 0, 1, \dots, M$, $T = 1 = Mk$, $\eta = 3$, $L + 1 = 3M$, $t_n = nk$, $n = 0, 1, \dots, 3M$.

For $j = 0, 1, \dots, M$, the discretization of the exact initial data is denoted $g_j = g(x_j)$ and its measured approximation $g_m(x_j)$ is simulated by adding random errors to $g(x_j)$. Specifically,

$$g_m(x_j) = g(x_j) + \epsilon_j,$$

where the ϵ_j 's are Gaussian random variables with variance $\sigma^2 = \epsilon^2$.

The discretized measured boundary data $\psi_m(t_n)$ and $\phi_m(t_n)$ are obtained in a similar way from the discrete versions of the exact functions $\psi(t)$ and $\phi(t)$, respectively.

To test the stability and accuracy of the numerical scheme, we use different average perturbations ϵ and appropriate values for the regularization parameters γ and δ . The errors in $a(x)$ and $u(x, t)$ are measured by the weighted- l^2 norms

$$|\Delta A|_2 \equiv \left[\frac{1}{M} \sum_{j=0}^{M-1} |a_{j+1/2} - A_{j+1/2}|^2 \right]^{1/2} \quad (15)$$

and

$$|\Delta U|_2 \equiv \left[\frac{1}{M^2} \sum_{j=0}^{M-1} \sum_{n=1}^M |u(jh, nk) - U_j^n|^2 \right]^{1/2} \quad (16)$$

respectively.

EXAMPLE 1. (Ewing and Lin, [3]). Identify $a(x)$ and $u(x, t)$ in

$$\begin{aligned} u_t &= (au_x)_x - (x^2 + 2x) \exp(x + t), & 0 < x < 1, 0 < t, \\ u(x, 0) &= \exp(x), & 0 < x < 1, \\ u(0, t) &= \exp(t), & 0 < t, \\ u_x(0, t) &= \exp(t), & 0 < t. \end{aligned} \quad (17)$$

The exact solutions are

$$a(x) = 1 + x^2 \quad \text{and} \quad u(x, t) = \exp(x + t).$$

Table 1 shows the discrete error norms, computed according to (15), as functions of the amount of noise in the data ϵ . The qualitative behavior of the reconstructed functions are shown in Figures 1 and 2.

Table 1. Error norms as functions of ϵ .

| Example 1 | | | Error Norms | |
|------------|----------|----------|----------------|----------------|
| ϵ | γ | δ | $ \Delta A _2$ | $ \Delta U _2$ |
| 0.000 | 0.050 | 0.000 | 0.002 | 0.000 |
| 0.003 | 0.100 | 0.020 | 0.058 | 0.014 |
| 0.005 | 0.100 | 0.030 | 0.054 | 0.014 |

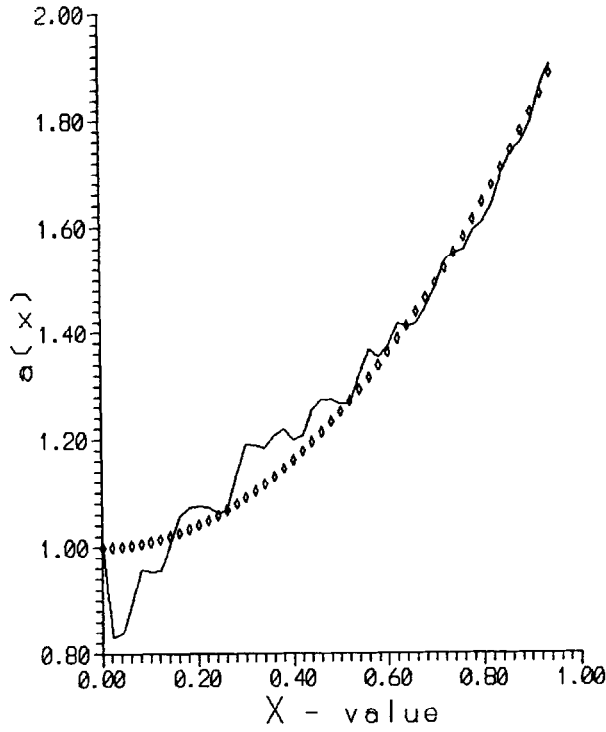


Figure 1. Reconstructed coefficient $a(x)$ in Example 1.

$\gamma = 0.1, \quad \epsilon = 0.005, \quad \delta = 0.03.$

Exact solution: ($\diamond\diamond\diamond$); Computed solution: (—).

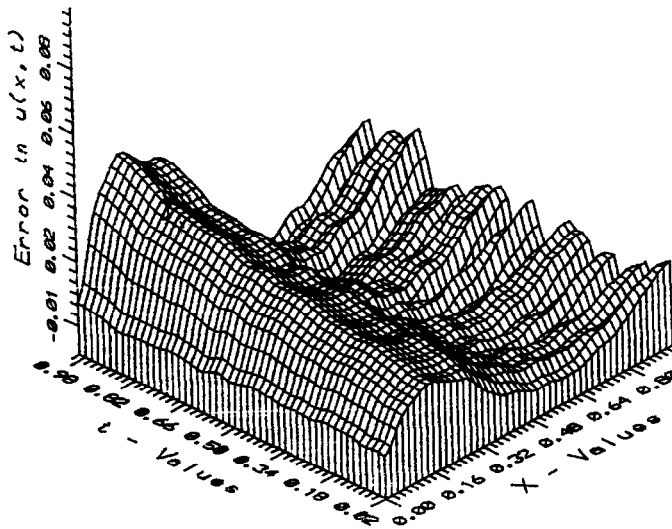


Figure 2. Error $|\Delta U|_2$ in the reconstruction of $u(x, t)$ in Example 1.

$\gamma = 0.1, \quad \epsilon = 0.005, \quad \delta = 0.03.$

EXAMPLE 2. In this example $u(0,0) = 0$ and $g'(x) = 1$ for all x . Recalling Assumption 1, we have $M_0 = M_1$. Hence $J_\delta g'$ and $(J_\delta g_m)'$ cannot satisfy the conditions of Assumption 1, making this example an important challenge for the numerical method. The identification problem is:

Identify $a(x)$ and $u(x, t)$ in

$$\begin{aligned} u_t &= (au_x)_x + f(x+t), & 0 < x < 1, 0 < t, \\ u(x, 0) &= x, & 0 < x < 1, \\ u(0, t) &= t \exp(t), & 0 < t, \\ u_x(0, t) &= \exp(-t) + t \exp(t), & 0 < t, \end{aligned} \tag{18}$$

where

$$f(x, t) = -(x + 0.01) \exp(-t) + \exp(x + t) - 0.01(x + 1)t \exp(x + t).$$

The exact solutions are

$$a(x) = 1 + 0.01x \quad \text{and} \quad u(x, t) = x \exp(-t) + t \exp(x + t).$$

Table 2 illustrates the stability of the method by showing the errors as functions of the amount of noise ϵ . The quality of the reconstructions can be observed in Figures 3 and 4.

Table 2. Error norms as functions of ϵ .

| Example 2 | | | Error Norms | |
|------------|----------|----------|----------------|----------------|
| ϵ | γ | δ | $ \Delta A _2$ | $ \Delta U _2$ |
| 0.000 | 0.100 | 0.000 | 0.019 | 0.005 |
| 0.003 | 0.100 | 0.030 | 0.076 | 0.021 |
| 0.005 | 0.100 | 0.030 | 0.080 | 0.019 |

EXAMPLE 3. (EWING AND LIN, [3]). This example consists of the reconstruction of a coefficient $a(x)$ that is only piecewise differentiable.

Identify $a(x)$ in

$$\begin{aligned} u_t &= (au_x)_x + f(x+t), & 0 < x < 1, 0 < t, \\ u(x, 0) &= \exp(x), & 0 < x < 1, \\ u(0, t) &= \exp(t), & 0 < t, \\ u_x(0, t) &= \exp(t), & 0 < t, \end{aligned} \tag{19}$$

where

$$f(x, t) = \begin{cases} \frac{1}{2} \exp(x+t), & 0 \leq x \leq \frac{1}{3}, \\ -\left(\frac{3}{2} + 3x\right) \exp(x+t), & \frac{1}{3} \leq x \leq \frac{1}{2}, \\ \left(\frac{3}{2}x + \frac{3}{4}\right) \exp(x+t), & \frac{1}{2} \leq x \leq \frac{2}{3}, \\ \frac{1}{4} \exp(x+t), & \frac{2}{3} \leq x \leq 1. \end{cases}$$

The exact coefficient is the non-smooth function

$$a(x) = \begin{cases} \frac{1}{2}, & 0 \leq x \leq \frac{1}{3}, \\ 3x - \frac{1}{2}, & \frac{1}{3} \leq x \leq \frac{1}{2}, \\ -\frac{3}{2}x + \frac{7}{4}, & \frac{1}{2} \leq x \leq \frac{2}{3}, \\ \frac{3}{4}, & \frac{2}{3} \leq x \leq 1. \end{cases}$$

Table 3 and Figure 5 illustrate the stability and accuracy of the reconstruction of this challenging coefficient.

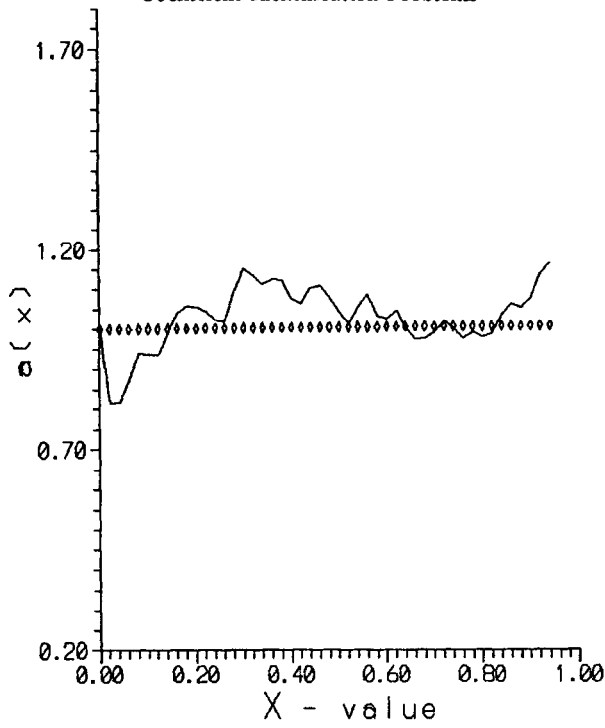


Figure 3. Reconstructed coefficient $a(x)$ in Example 2.

$\gamma = 0.1, \quad \epsilon = 0.005, \quad \delta = 0.03.$

Exact solution: ($\diamond \diamond \diamond$); Computed solution: ($-$).

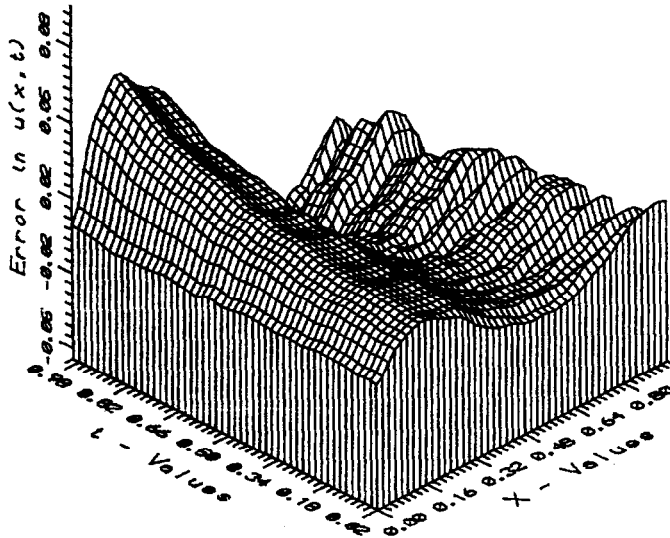


Figure 4. Error $|\Delta U|_2$ in the reconstruction of $u(x, t)$ in Example 2.

$\gamma = 0.1, \quad \epsilon = 0.005, \quad \delta = 0.03.$

Table 3. Error norms as functions of ϵ .

| Example 3 | | | Error Norms | |
|------------|----------|----------|----------------|----------------|
| ϵ | γ | δ | $ \Delta A _2$ | $ \Delta U _2$ |
| 0.000 | 0.080 | 0.000 | 0.004 | 0.000 |
| 0.003 | 0.120 | 0.030 | 0.026 | 0.013 |
| 0.005 | 0.120 | 0.030 | 0.029 | 0.017 |

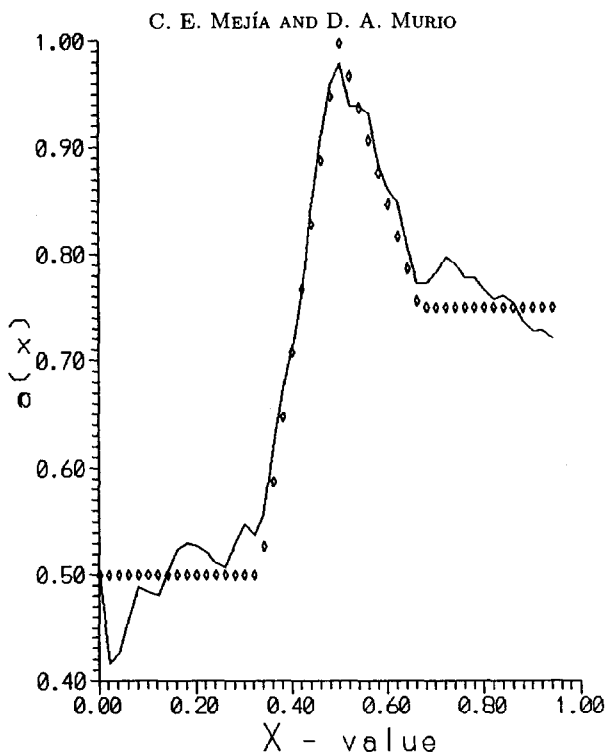


Figure 5. Reconstructed coefficient $a(x)$ in Example 3.

$$\gamma = 0.12, \quad \epsilon = 0.005, \quad \delta = 0.03.$$

Exact solution: ($\diamond \diamond \diamond$); Computed solution: (—).

REFERENCES

1. G. Chavent and J. Jaffré, *Mathl. Models and Finite Elements for Reservoir Simulation*, North-Holland, Amsterdam, (1986).
2. M.F. Wheeler, Ed., *Numerical Simulation in Oil Recovery*, Springer-Verlag, New York, (1988).
3. R. Ewing and T. Lin, Parameter identification problems in single-phase and two-phase flow, In *International Series of Numerical Mathematics*, pp. 85–108, Birkhäuser Verlag, Basel, (1989).
4. R. Ewing, T. Lin and R. Falk, Inverse and ill-posed problems in reservoir simulation, In *Inverse and Ill-Posed Problems*, (Edited by H.W. Engl and C.W. Groetsch), pp. 483–497, Academic Press, Orlando, (1987).
5. D.A. Murio, *The Mollification Method and the Numerical Solution of Ill-Posed Problems*, John Wiley, New York, (1993).
6. C.F. Weber, Analysis and solution of the ill-posed inverse heat conduction problem, *Int. J. Heat Mass Transfer* **24**, 1783–1792 (1981).
7. D.A. Murio and C. Roth, An integral solution for the inverse heat conduction problem after the method of Weber, *Computers Math. Applic.* **15** (1), 39–51 (1988).
8. D.A. Murio, Automatic numerical differentiation by discrete mollification, *Computers Math. Applic.* **13** (4), 381–386 (1987).